Abdominal Radiology (2019) 44:2759–2768
https://doi.org/10.1007/s00261-019-02036-w

HEPATOBILIARY

Consistency of hepatocellular gadoxetic acid uptake in serial MRI examinations for evaluation of liver function

Dorothea Theilig[1] · Aboelyazid Elkilany[1] · Moritz Schmelzle[2] · Tobias Müller[3] · Bernd Hamm[1] · Timm Denecke[1] · Dominik Geisel[1]

Published online: 25 April 2019

Abstract

Purpose To assess the consistency of liver enhancement in gadoxetic acid-enhanced magnetic resonance imaging (MRI) over serial examinations.

Methods This retrospective study included 554 patients who underwent at least 2 serial gadoxetic acid-enhanced MRI scans at either 1.5 or 3.0 Tesla at our institution between 2014 and 2018. Signal intensities (SI) were measured on T1-weighted images before and approx. 20 min after intravenous injection of gadoxetic acid. Relative enhancement (RE) of the liver, liver-to-spleen SI ratio (LSR), and liver-to-muscle SI ratio (LMR) were calculated. Means were compared with the paired *t* test, Greenhouse–Geisser test, and linear mixed model analysis, accordingly. Multiple linear regression analysis was used to elucidate possible predictors of RE and bivariate correlation analysis of patient age with RE was performed.

Results No statistically significant difference in RE, LSR, and LMR between two consecutive MRI scans was found when tested with paired *t* test or Greenhouse–Geisser test ($n = 554$, 519, and 554, respectively), while the latter revealed a statistically significant difference between the first and fourth MRI scan which was not confirmed in the linear mixed model. Patient age correlated negatively with RE of the liver ($p = 0.002$), LSR ($p < 0.001$), and LMR ($p = 0.006$).

Conclusions Relative enhancement of the liver in the hepatobiliary phase of gadoxetic acid-enhanced MRI is consistent over successive examinations, different scanner types, and field strengths while correlating negatively with age, which further underscores the validity of gadoxetic acid-enhanced MRI as an imaging-based liver function test.

Keywords Liver · Magnetic resonance imaging · Contrast agent

✉ Dorothea Theilig
dorothea.theilig@charite.de

Aboelyazid Elkilany
aboelyazid.elkilany@charite.de

Moritz Schmelzle
moritz.schmelzle@charite.de

Tobias Müller
tobias.mueller@charite.de

Bernd Hamm
bernd.hamm@charite.de

Timm Denecke
timm.denecke@charite.de

Dominik Geisel
dominik.geisel@charite.de

[1] Department of Diagnostic and Interventional Radiology, Charité – Universitätsmedizin Berlin, corporate member of Freie Universität Berlin, Humboldt-Universität zu Berlin, Augustenburger Platz 1, 13353 Berlin, Germany

[2] Department of General, Visceral and Transplantation Surgery, Charité – Universitätsmedizin Berlin, corporate member of Freie Universität Berlin, Humboldt-Universität zu Berlin, Augustenburger Platz 1, 13353 Berlin, Germany

[3] Division of Hepatology and Gastroenterology, Medical Department, Charité – Universitätsmedizin Berlin, corporate member of Freie Universität Berlin, Humboldt-Universität zu Berlin, Augustenburger Platz 1, 13353 Berlin, Germany

Introduction

Liver-specific uptake of gadolinium ethoxybenzyl diethylenetriamine pentaacetic acid (gadoxetic acid) after intravenous administration is the rationale for using this contrast agent as an imaging-based liver function test [1]. The validity of this test has been verified in comparison with the available global liver function tests such as liver enzyme blood tests, clinical and biochemical grading schemes like the Child–Pugh classification and the Model for End-Stage Liver Disease (MELD) score, dynamic liver function tests such as the indocyanine green (ICG) plasma disappearance rate and the less widely used C-methacetin breath test (LIver MAXimum function capacity, LiMAx, Humedics GmbH, Berlin, Germany) as well as with other imaging-based liver function tests such as ^{99m}Tc GSA scintigraphy [2–10]. Easy integration into clinical work-up, absence of ionizing radiation, and above all the possibility of obtaining information on the special distribution of liver function has led to an increasing appreciation of the advantage that gadoxetic acid-enhanced MRI as an imaging-based liver function test has over global liver function tests and scintigraphy. Prediction of future liver remnant function after portal vein embolization is just one more recent example of the benefit of gadoxetic acid-enhanced MRI for imaging-based evaluation of liver function [11].

There are several options to measure the T1-shortening effect of gadoxetic acid including T1-relaxometry-derived indices and signal intensity-based indices with signal intensities determined either relative to unenhanced images or in comparison to reference tissue without specific transporter-mediated uptake of gadoxetic acid such as spleen or muscle. This is necessary because MRI signal intensity is not absolute and hepatocellular uptake cannot be distinguished from residual blood pool enhancement [10, 12–16].

However, all these measurements might be influenced by a variety of factors, not only related to imaging parameters such as scanner type, field strength, or amount of contrast agent administered but also related to patient characteristics such as physiological differences due to age [17].

The aim of this study was to assess the consistency of gadoxetic acid-enhanced MRI as a liver function test across serial examinations and different MRI scanners. The principal assumption of this study was that over short time periods, liver function in regions without tumor infiltration can be expected to stay rather stable when having excluded patients with signs of decompensated liver disease from the study. Repeat examinations performed within short time intervals can therefore be used to evaluate consistency of gadoxetic acid-enhanced MRI and to identify external factors that may affect uptake of the contrast agent.

Materials and methods

Patient population and study design

We retrospectively retrieved all patients who had undergone a series of at least two gadoxetic acid-enhanced MRI examinations at our department between August 1, 2014 and April 4, 2018. A total of 1,116 patients met this criterion. From these patients, we subsequently excluded all those that showed signs of decompensated liver disease such as ascites or obvious varices on imaging studies, that had previous locoregional interventional treatments for liver tumors (534), previous portal vein embolization (13), transjugular intrahepatic portosystemic shunt (TIPS), liver transplant after the first MRI study (2), or technical problems during the examination resulting in incomplete MRI (13). Patients with previous liver surgery, on the other hand, were not excluded as the resulting defects are clear cut, i.e., simply missing, and can therefore not be inadvertently used for signal intensity measurements unlike in patients with locoregional interventional treatments which might have a morphologically not discernable effect on liver parenchyma elsewhere. This left a total of 554 patients for the analysis of this study. The indications for the MRI scans in these patients can be divided into six categories:

1. Neuroendocrine tumors affecting the liver: evaluation, staging, and follow-up after therapy (systemic chemotherapy or surgery).
2. Hepatic metastasis from extrahepatic primary: evaluation, staging, and follow-up after therapy (systemic chemotherapy or surgery).
3. Indeterminate focal hepatic lesions: characterization and follow-up.
4. Cirrhotic liver: monitoring for detection and characterization of focal hepatic lesions in cirrhotic liver.
5. Primary hepatic malignancy: evaluation, staging, and follow-up examination after therapy (systemic chemotherapy or surgery)
6. Diffuse liver disease: evaluation and follow-up.

In the population of 554 patients included in our analysis, 151 had cirrhosis, 238 underwent chemotherapy, and 42 had liver surgery after the first MRI. Prior to the first MRI examination analyzed in this retrospective setting, 90 patients had liver surgery, 11 patients underwent liver transplant, 3 patients received a transjugular intrahepatic portosystemic shunt, and 35 patients had splenectomy. Patient characteristics are summarized in Table 1. The retrospective study was approved by the institutional review board, informed consent was waived.

Table 1 Descriptive statistics of the study population

	MRI 1	MRI 2	MRI 3	MRI 4
N (LSR/LMR/T1RR/Bilirubin)	554 (519/554/26/334)	554 (516/554/26/326)	255 (230/255/5/124)	137 (118/137/2/61)
Time to previous MRI in days (95% confidence interval)	–	229 ± 202 (212.5–246.1)	198 ± 133 (108.8–212.5)	191 ± 114 (171.9–210.2)
Age in years	58 ± 14	58 ± 24	59 ± 14	59 ± 15
Gender (m/f)	298/256	298/256	131/124	69/68
Bilirubin (mg/dl)	0.56 ± 0.08	0.68 ± 0.17	0.53 ± 0.13	0.67 ± 0.18
Cirrhosis	151 (27%)	151 (27%)	51 (20%)	15 (11%)
Chemotherapy	238 (43%)	238 (43%)	139 (55%)	92 (67%)
Surgery after MRI 1	42 (8%)	42 (8%)	17 (7%)	10 (7%)
Indication for MRI				
1. Neuroendocrine tumor affecting the liver	216 (39%)	216 (39%)	145 (57%)	99 (72%)
2. Hepatic metastasis	111 (20%)	111 (20%)	38 (15%)	16 (12%)
3. Indeterminate focal hepatic lesions	23 (4%)	23 (4%)	6 (2%)	1 (1%)
4. Monitoring cirrhotic liver	44 (8%)	44 (8%)	16 (6%)	8 (6%)
5. Primary hepatic malignancy	121 (22%)	121 (22%)	39 (15%)	12 (9%)
6. Diffuse liver disease	39 (7%)	39 (7%)	11 (4%)	1 (1%)
MRI field strength (1.5T/3.0T)	429 (78%)/125 (22%)	456 (82%)/98 (18%)	214 (84%)/41(16%)	113 (82%)/24 (18%)
Scanner type (1/2/3/4)	87/276/66/125	131/272/53/98	55/145/14/41	23/75/15/24
Amount of contrast agent (ml)	7.8 ± 1.4	7.8 ± 1.4	7.9 (± 1.4)	7.9 (± 1.4)
RE	0.660 ± 0.219	0.6445 ± 0.215	0.660 ± 0.178	0.668 ± 0.164
LSR	1.718 ± 0.369	1.749 ± 0.641	1.823 ± 1.200	1.752 ± 0.298
LMR	2.203 ± 0.420	2.218 ± 0.416	2.253 ± 0.404	2.256 ± 0.347
T1RR	66.83 ± 12.01	64.85 ± 13.96	62.99 ± 8.28	68.85 ± 3.44
Delay of hepatobiliary phase (min)	17 ± 4	17 ± 4	17 ± 3	17 ± 3

LSR liver-to-spleen ratio of signal intensity in gadoxetic acid-enhanced MRI, *LMR* liver-to-muscle ratio of signal intensity in gadoxetic acid-enhanced MRI, *T1RR* T1 reduction rate, *RE* relative enhancement. Scanner type 1: 1.5T Siemens Magnetom Avanto, scanner type 2 and 3: 1.5T Siemens Magnetom Aera, scanner type 4: 3.0T Siemens Magnetom Skyra

MRI

MRI examinations were performed at three different types of scanners, 1.5 T Siemens Magnetom Avanto, 1.5 T Siemens Magnetom Aera, and 3.0 T Siemens Magnetom Skyra (Siemens Healthcare, Erlangen, Germany)—using an eight-channel body phased-array coil. Transverse T1-weighted images (volume-interpolated breath-hold examination (VIBE) sequence covering the entire liver with 60–80 slices and an adjusted field of view of 255–300 × 340–400 mm) were acquired before and approximately 20 min after manual intravenous bolus injection of 0.1 ml per kg body weight of gadoxetic acid (Primovist, Bayer Pharma, Berlin, Germany).

Imaging parameters at 1.5 T were as follows: repetition time (TR) of 4.58 ms, echo time (TE) of 2.25 ms, flip angle (FA) of 9°, slice thickness of 3 mm, and matrix size of 276 × 340. Imaging parameters at 3.0 T were as follows: repetition time (TR) of 4.25 ms, echo time (TE) of 2.07 ms, flip angle (FA) of 9°, slice thickness of 3 mm, and matrix size of 276 × 340.

In some patients, T1 mapping sequences were acquired: T1 maps were calculated using the MapIt software package for Syngo vers. E11 (Siemens). The comprehensive sequence software solution consists of B1 mapping to measure spatial flip angle distribution and T1 mapping using a flip angle variation method with B1-corrected flip angles. B1 maps were generated using a double-angle method (8°/80° FA, 375 × 305 × 288 mm FOV, 64 × 52 matrix, 18 slices, 8 mm slice thickness, 24 mm slice distance, 5050 ms TR (acquisition duration for one FA), and 1.83 ms TE) based on a 2D gradient-echo sequence (2D-TurboFlash/2D-GRE). T1 times were calculated using a double-angle method (3°/15° FA, 380 × 305 × 256 mm FOV, 256 × 156 acquisition matrix, 448 × 360 image matrix, 64 slices, 5.01 ms TR, 4788 ms acquisition duration for one FA, 2.3 ms TE) based on a 3D gradient-echo sequence (3D-TurboFlash/3D-GRE) and the corrected flip angle distribution from the B1 map calculated before.

Image analysis

All MRI scans were reviewed by a single reader with 10 years of experience in abdominal imaging and MRI who was blinded to liver function. Images were analyzed using the Visage 7.1.11 software (Visage Imaging, Richmond, NSW, Australia). Signal intensity (SI) was measured in three regions of interest (ROI) with approximately 2.5 cm diameter prior to (SI unenhanced) and approximately 20 min after intravenous bolus injection of gadoxetic acid, i.e., in the hepatobiliary phase (SI in hepatobiliary phase) placing one ROI in segment V/VIII, one ROI in segment VI/VII, and one ROI in the left lobe. Large vessels, bile ducts, and tumor masses were avoided. In follow-up MRIs, ROIs were placed in the same regions. Relative enhancement (RE) of the liver was calculated with the following formula:

$$\text{RE} = (\text{SI in hepatobiliary phase} - \text{SI unenhanced})/\text{SI unenhanced}$$

Signal intensity (SI) of the liver was compared to that of tissue without transporter-mediated cellular gadoxetic acid uptake, i.e., paravertebral muscle and spleen. Liver-to-muscle ratio (LMR) and liver-to-spleen ratio (LSR) of SI were calculated as follows:

$$\text{LMR} = \text{liver SI in hepatobiliary phase/muscle SI in hepatobiliary phase}$$

$$\text{LSR} = \text{liver SI in hepatobiliary phase/spleen SI in hepatobiliary phase}$$

When T1 mapping sequences were available, the T1 reduction rate (T1RR) was calculated using the following formula:

$$\text{T1RR} = ((\text{T1 unenhanced} - \text{T1 in hepatobiliary phase})/\text{T1 unenhanced}) \times 100\,(\%)$$

Statistics

Continuous variables are presented as mean ± standard deviation (SD). Bivariate analysis was used for simple correlation analysis. Multiple linear regression analysis was used to elucidate possible predictors of the outcome parameters. Differences between two groups were assessed with the Mann–Whitney U-test (MWU) and paired *t* test. linear mixed model with compound symmetry covariance matrix and timepoint of MRI serving as fixed variable and Greenhouse–Geisser test were used for repeated measurements. Power analysis of the paired-test was performed using G*Power 3.1 [18]. All other statistical analysis was performed with SPSS Statistics 25 (IBM, Armonk, NY, USA). A p value of < 0.05 was considered statistically significant.

Results

The principal assumption of the study that over the short time periods that elapsed between the MRIs liver function in regions without tumor infiltration can be expected to stay rather stable in the study population was underscored by the fact that bilirubin values available at the different timepoints did not differ significantly from each other (Table 1, 2 and 3).

The major aim of the study to confirm the reproducibility of gadoxetic acid-enhanced MRI as an imaging-based liver function test was subsequently achieved:

In our study population of 554 patients, no statistically significant difference in RE and LMR between the first and second gadoxetic acid-enhanced MRI scan was found when tested with the paired *t* test that was shown to have a statistical power of 78% in post hoc analysis. Also, no statistically significant difference between the first and second gadoxetic acid-enhanced MRI examination was found for LSR in a smaller population of $n = 519$ (due to splenectomy) or for T1RR in a very small subset of $n = 26$; see Table 2.

Repeated-measures analysis of patients with a series of at least 2 gadoxetic acid-enhanced MRI examinations also showed no statistically significant difference between any two consecutive MRI scans when tested with the Geisser test but a tendency of a gradual decrease in RE, LSR, and LMR over a longer period of time, resulting in a statistically significant difference between the first and fourth MRI scan with $p = 0.006$ for RE and $p = 0.019$ for LSR; see Fig. 1 and Table 3. Note that the described gradual decrease in

Table 2 Comparison of signal intensity measurements of the liver in repeated gadoxetic acid-enhanced MRI as well as the Bilirubin values at the same timepoints using the paired *t* test

	n	MRI 1	MRI 2	Sig. of paired *t* test
RE	554	0.660 ± 0.219	0.6445 ± 0.215	0.085
LSR	516	1.717 ± 0.370	1.749 ± 0.641	0.266
LMR	554	2.203 ± 0.420	2.218 ± 0.416	0.386
T1RR	26	66.83 ± 12.01	64.85 ± 13.96	0.198
Bilirubin	199	1.04 ± 2.67	1.02 ± 1.43	0.343

Table 3 Comparison of signal intensity measurements of the liver in serial gadoxetic acid-enhanced MRI examinations using the Greenhouse–Geisser test and comparison of bilirubin values at the corresponding timepoints with linear mixed model with compound symmetry covariance matrix and timepoint of MRI serving as fixed variable

	Greenhouse–Geisser test		Linear mixed model							
	n	Sig.	*n*	Sig.	Sig. of pairwise comparison					
					MRI 1 to 2	MRI 1 to 3	MRI 1 to 4	MRI 2 to 3	MRI 2 to 4	MRI 3 to 4
RE	137	0.013*	554	0.060	0.470	0.416	0.121	1.000	1.000	1.000
LSR	118	0.050*	519	0.351	1.000	0.441	1.000	1.000	1.000	1.000
LMR	137	0.263	554	0.636	1.000	1.000	1.000	1.000	1.000	1.000
T1RR	–	–	44	0.474	1.000	0.808	1.000	1.000	1.000	1.000
RE of patients w/cirrhosis	51	0.242	151	0.822	1.000	1.000	1.000	1.000	1.000	1.000
RE of patients w/chemotherapy	139	0.021*	238	0.029*	0.390	0.473	0.030*	1.000	0.777	1.000
RE of patients w/surgery after MRI 1	42	0.039*	168	0.168	0.380	1.000	1.000	0.410	1.000	1.000
RE of patients w/o chemotherapy or surgery after MRI 1	108	0.053	297	0.676	1.000	1.000	1.000	1.000	1.000	1.000
Bilirubin	61	0.276	450	0.350	0.625	1.000	1.000	1.000	1.000	1.000

For subgroup analysis, the number of repeated MRI examinations compared was limited to 2 or 3 in order not to reduce the number (*n*) below a statistically reasonable threshold, which accounts for the empty boxes in this table. *Indicates a statistically significant difference ($p < 0.05$)

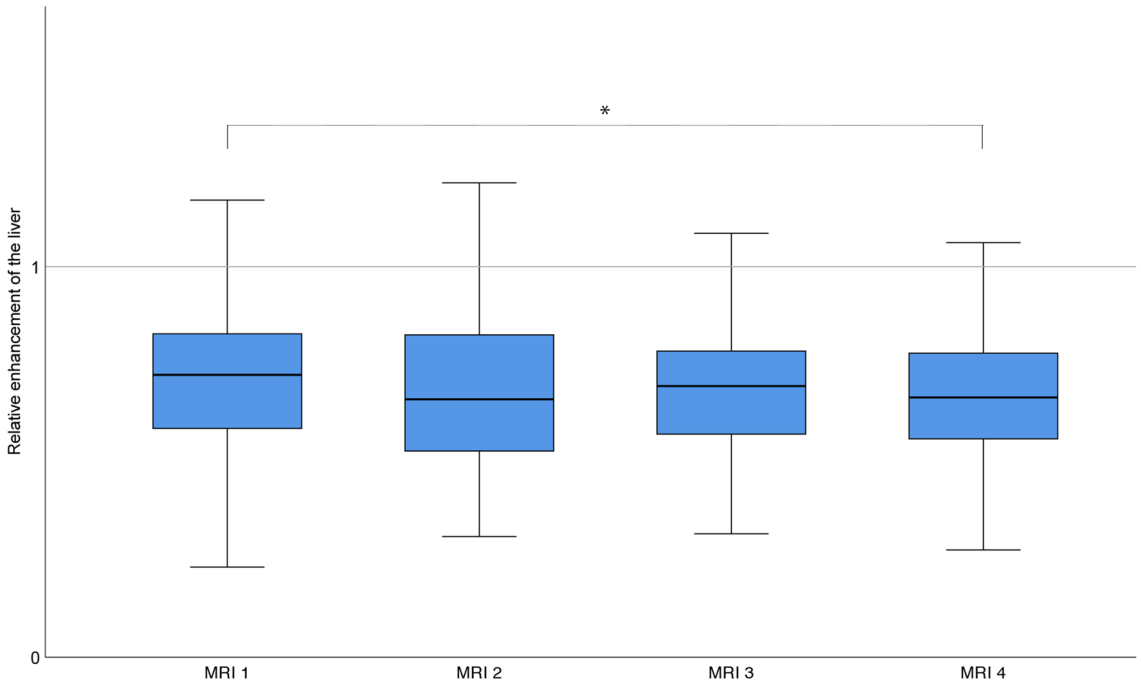

Fig. 1 Boxplot diagram depicting distribution of relative enhancement (RE) of the liver on gadoxetic acid-enhanced MRI of consecutive MRI examinations, numbered 1 to 4. Number (n) of patients included = 137. *Indicates a statistically significant difference ($p < 0.05$) in Greenhouse–Geisser test which was not confirmed in the linear mixed model analysis

RE over the longer period of time is not apparent in the results presented in Table 1 as the means given there include all patients who had an MRI at the respective timepoints, whereas the repeated-measures analysis showing the decrease only includes those patients at previous timepoints who also underwent all subsequent scans that were included in the analysis, compare numbers (*n*) given in Table 3.

Subgroup analysis of the patient population revealed that patients who underwent chemotherapy had a statistically significant decrease in RE whereas patients without

chemotherapy including those who underwent MRI for cirrhosis showed no statistically significant difference in RE between MRI scans; see Table 3.

Regarding factors affecting contrast uptake in general, multiple linear regression analysis showed that only age, cirrhosis and bilirubin value were statistically significant predictors of relative enhancement of the liver (Table 4).

Patient age was found to correlate negatively with RE of the liver (Pearson correlation coefficient = − 0.130, $p = 0.002$) as well as with LSR (Pearson correlation coefficient = − 0.220, $p < 0.001$) and LMR (Pearson correlation coefficient = − 0.117, $p = 0.006$). This correlation was more marked when only taking patients without cirrhosis into account (Pearson correlation coefficient − 0.215, − 0.299 and − 0.118, respectively, and $p < 0.001$), see Table 5 and Fig. 2.

Analysis of liver RE in relation to the amount of contrast agent administered in the first MRI revealed a negative correlation, i.e., the more contrast agent administered the less the RE of the liver (Pearson correlation coefficient − 0.156, $p < 0.001$); see Fig. 3.

An interesting secondary finding of this analysis was a statistically significant greater RE of the liver, LSR and LMR in women compared with men ($p < 0.001$), which remained statistically significant with $p < 0.001$, $p = 0.024$ and $p = 0.001$, respectively, when only taking patients without cirrhosis into account; see Table 6.

Analysis of the impact of individual delays of the hepatobiliary phase acquisition, which ranged from 7 to 40 min with a mean of 17 min and a standard deviation of ± 4 min (see Table 1), identified no statistically significant correlation with RE, LSR or LMR ($n = 554$ and $p = 0.10$, $n = 519$ and $p = 0.93$, $n = 554$ and $p = 0.91$, respectively).

Discussion

In our study we found that RE of the liver on gadoxetic acid-enhanced MRI is consistent and reproducible over short periods of time and across different scanner types (Siemens Magnetom Avanto, Siemens Magnetom Aera, and Siemens Magnetom Skyra) and field strengths (1.5 T and 3.0 T). This major finding of the study provides further evidence that gadoxetic acid-enhanced MRI can be used as an imaging-based liver function test in routine clinical practice. This is of great clinical impact as gadoxetic acid-enhanced MRI has several advantages over global liver function test, most importantly the fact that it allows determination of regional distribution of liver function and that it is easily integrated into clinical routine while not involving ionizing radiation.

Table 4 Results of multiple linear regression analysis with relative enhancement (RE) in MRI 1 and relative chance in RE between MRI 1 and MRI 2 as a dependent variable, the model showed a coefficient of determination (R^2) of 0.272 for the former and 0.042 for the latter

	RE in MRI 1		Relative change in RE between MRI 1 and MRI 2	
Independent variable	B (95% CI)	*p* value	B (95% CI)	*p* value
Gender	0.034 (− 0.034; 0.065)	0.533	0.093 (− 0.031; 0.222)	0.139
Age	− 0.102 (− 0.003; 0.000)	0.039*	0.061 (− 0.002; 0.006)	0.280
Indication for MRI	0.098 (− 0.004; 0.029)	0.152	− 0.099 (− 0.070; 0.015)	0.209
Amount of contrast agent	− 0.076 (− 0.028; 0.005)	0.158	0.023 (− 0.035; 0.051)	0.711
Time to hepatobiliary phase	0.074 (− 0.001; 0.010)	0.123	− 0.045 (− 0.020; 0.008)	0.415
Cirrhosis	− 0.372 (− 0.001; 0.010)	0.000*	0.137 (− 0.010; 0.305)	0.066
Chemotherapy	0.003 (− 0.052; 0.055)	0.964	− 0.040 (− 0.178; 0.097)	0.564
Surgery after MRI 1	0.014 (− 0.062; 0.082)	0.778	− 0.078 (− 0.316; 0.055)	0.166
Surgery before MRI 1	− 0.073 (− 0.104; 0.014)	0.137	0.039 (− 0.098; 0.205)	0.488
Bilirubin value	− 0.339 (− 0.040; − 0.022)	0.000*	0.081 (− 0.006; 0.039)	0.154

*Indicates a statistically significant difference ($p < 0.05$)

Table 5 Bivariate correlation of RE, LSR, LMR, and T1RR in gadoxetic acid-enhanced MRI and patient age

	All patients			Patients without cirrhosis		
	n	Pearson	*p* value	*n*	Pearson	*p* value
RE	554	− 0.130	0.002*	403	− 0.215	< 0.001*
LSR	519	− 0.220	< 0.001*	368	− 0.299	< 0.001*
LMR	554	− 0.117	0.006*	403	− 0.188	< 0.001*
T1RR	26	− 0.034	0.870	20	− 0.169	0.475

*Indicates a statistically significant difference ($p < 0.05$)

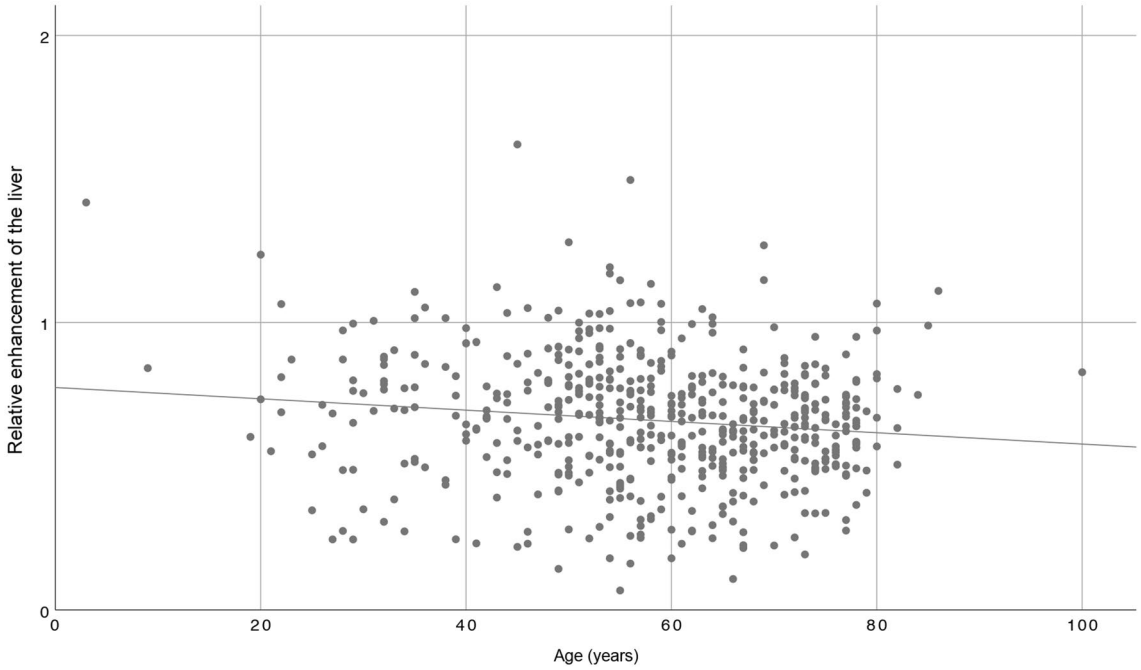

Fig. 2 Bivariate correlation of patient age with relative enhancement (RE) of the liver on gadoxetic acid-enhanced MRI. Number (*n*) of patients = 554; Pearson correlation coefficient − 0.130, $p = 0.002$

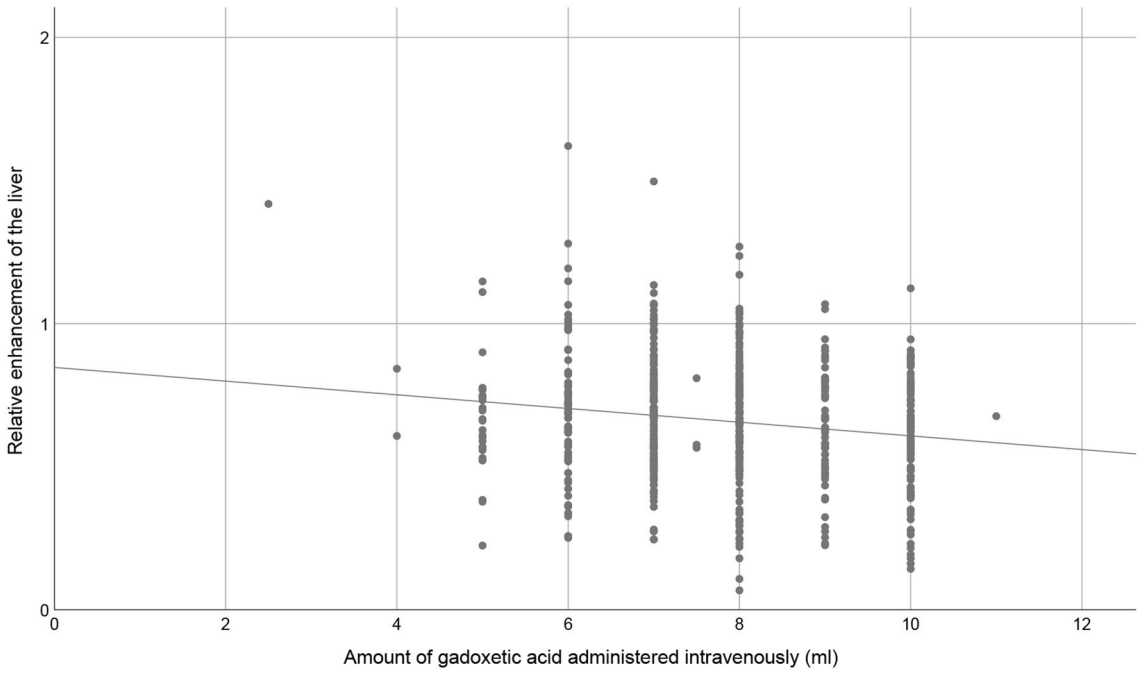

Fig. 3 Bivariate correlation of amount of gadoxetic acid administered intravenously with relative enhancement (RE) of the liver on gadoxetic acid-enhanced MRI. Number (*n*) of patients = 554; Pearson correlation coefficient − 0.156, $p < 0.001$

Not surprisingly, liver RE gradually decreased in the subset of study patients with serial MRI over a longer period of time. Further analysis of the patient population revealed that patients who underwent hepatic surgery between consecutive MRI examinations deteriorated in liver function, as did those who received chemotherapy. The former is a finding

Table 6 Mann–Whitney U-test (MWU) for comparison of RE, LSR, LMR, and T1RR in gadoxetic-enhanced MRI between men and women

	All patients					Patients without cirrhosis				
	Male		Female		MWU *p* value	Male		Female		MWU *p* value
	n	Mean ± SD	*n*	Mean ± SD		*n*	Mean	*N*	Mean	
RE	298	0.620 ± 0.212	256	0.707 ± 0.217	< 0.001*	191	0.671 ± 0.198	212	0.743 ± 0.212	< 0.001*
LSR	280	1.656 ± 0.361	239	1.786 ± 0.368	< 0.001*	173	1.774 ± 0.325	195	1.850 ± 0.336	0.024*
LMR	298	2.134 ± 0.397	256	2.284 ± 0.432	< 0.001*	191	2.250 ± 0.346	212	2.357 ± 0.412	0.001*
T1RR	14	63.22 ± 15.29	12	71.04 ± 3.92	0.176	9	69.46 ± 7.13	11	70.87 ± 4.06	0.656

*Indicates a statistically significant difference ($p < 0.05$)

reported in previous studies and might be attributed to exposure of the liver to intraoperative stress due to the clamping procedure, perioperative stress, and comorbidities [19, 20]. The latter can readily be ascribed to the hepatotoxicity of many chemotherapeutic agents as well as systemic effects of progressive cancer.

In our study population, patient age correlated negatively with RE of the liver as well as with LSR and LMR, and this correlation was even more marked when only taking non-cirrhotic patients into account. This supports the findings obtained by Verloh et al. in a much smaller patient population ($n = 124$) [21]. Similar results were also reported by Matoori et al. although an impact of age on liver enhancement in their study was only seen when normalized to reference tissue such as spleen or erector spinae muscle, which might be partly due to an even smaller study population size ($n = 75$) [17]. While in our study over 500 patients were available for the analysis of the correlation of patient age with RE, LMR, and LSR, and due to splenectomy a slightly smaller number of $n = 519$ patients were available for correlation with LSR, unfortunately only 26 patients were examined with T1 mapping sequences. Therefore, our finding that T1RR did not correlate significantly with age in our study is most likely due to the small number of patients in this subgroup analysis. In fact, it is rather plausible that physiological changes associated with aging such as an altered hepatic drug metabolism, as described elsewhere [22], have an impact on liver function and therefore the changes in RE seen in our study.

Some of the secondary findings of our study are not self-explanatory at first glance. This is a statistically significant negative correlation between the amount of contrast agent administered intravenously and RE of the liver and a statistically significantly greater RE of the liver in women. A possible explanation for the negative correlation between the amount of contrast agent administered and liver RE in the hepatobiliary phase of gadoxetic acid-enhanced MRI might be that adapting the amount of contrast agent to body weight as routinely done at our institution (0.1 ml per kg body) might in fact be insufficient, i.e., it may be necessary to adjust the amount of contrast agent in an exponential rather than a linear fashion or to adapt the amount to liver volume rather than body weight. The latter is supported by the aforementioned study of Verloh et al., who found a significant impact of liver volume on RE [21]. Besides, the fact that it is clinical practice to not administer more than one syringe of gadoxetic acid (10 ml) per examination might have added to the described observation as this means that patients with a body weight of more than 100 kg do not receive enough contrast agent according to the linear body weight adaptation scheme currently propagated. The difference in liver RE between men and women, on the other hand, might be explained by the fact that women, on average, tend to weigh less than men and therefore receive less contrast agent on average according to the dosing scheme of 0.1 ml per kg body, so that the above-described negative correlation of amount of contrast agent and liver RE may simply be reflected in this subgroup analysis. On top of that, epidemiologically, the frequencies of various hepatic neoplasms differ between men and women [23], which is likely to result in different degrees of liver impairment, possibly adding to the differences observed in this subgroup analysis.

Limitations of study

The retrospective design is a limitation of our study. The principal assumption of this study was that over the short time periods that elapsed between the MRIs liver function in regions without tumor infiltration can be expected to stay rather stable in the study population as patients with signs of decompensated liver disease were initially excluded from the study. The possible exception here being patients who had been receiving chemotherapy at the time which is why this subgroup was analyzed separately as well. But even without excluding this subgroup bilirubin values available at the different timepoints did not differ significantly from each other underscoring the above-stated principal assumption of the study (Tables 1, 2, and 3). However, due to the retrospective design of the study, bilirubin values could not be retrieved

for all patients at all timepoints which constitutes a limitation of the study. We would like to point out, though, that there is no real gold standard with proven consistency for testing liver function. The widely used ICG plasma disappearance rate, for example, is known to vary with the degree of liver perfusion, which in turn depends on cardiac output [24, 25]. So basing the study on what we would argue to be a reasonable assumption might in fact be the better approach.

In current clinical practice, the amount of contrast agent administered is adapted to the body weight of the patient (0.1 ml per kg body) but generally does not exceed the amount of 10 ml contained in the commercially available syringes. This constitutes a potential limitation of the study. As the aim of this study was to analyze the reproducibility of gadoxetic acid-enhanced MRI as an imaging-based liver function test as currently performed in a routine clinical setting and not in a hypothetical optimized setting this could also be regarded as an advantage.

A further limitation of our study is that the number of patients examined with T1 mapping sequences was rather small, rendering the results of this subgroup analysis less valid. A prospective study comparing the consistency of gadoxetic acid-enhanced MRI with T1 mapping with signal intensity-based indices would be desirable.

Conclusions

Relative enhancement of the liver in the hepatobiliary phase of gadoxidic acid-enhanced MRI is consistent over successive examinations, scanner types, and field strengths while correlating negatively with age. This further underscores the validity of gadoxetic acid-enhanced MRI as an imaging-based liver function test.

Acknowledgements The authors thank Bettina Herwig for language editing.

References

1. L. Pascolo, F. Cupelli, P.L. Anelli, V. Lorusso, M. Visigalli, F. Uggeri, C. Tiribelli, Molecular mechanisms for the hepatic uptake of magnetic resonance imaging contrast agents, Biochem Biophys Res Commun 257(3) (1999) 746-52. https://doi.org/10.1006/bbrc.1999.0454
2. N. Verloh, M. Haimerl, F. Zeman, M. Schlabeck, A. Barreiros, M. Loss, A.G. Schreyer, C. Stroszczynski, C. Fellner, P. Wiggermann, Assessing liver function by liver enhancement during the hepatobiliary phase with Gd-EOB-DTPA-enhanced MRI at 3 Tesla, European radiology 24(5) (2014) 1013-9. https://doi.org/10.1007/s00330-014-3108-y.
3. M. Haimerl, N. Verloh, C. Fellner, F. Zeman, A. Teufel, S. Fichtner-Feigl, A.G. Schreyer, C. Stroszczynski, P. Wiggermann, MRI-based estimation of liver function: Gd-EOB-DTPA-enhanced T1 relaxometry of 3T vs. the MELD score, Sci Rep 4 (2014) 5621. https://doi.org/10.1038/srep05621.
4. A. Yamada, T. Hara, F. Li, Y. Fujinaga, K. Ueda, M. Kadoya, K. Doi, Quantitative evaluation of liver function with use of gadoxetate disodium-enhanced MR imaging, Radiology 260(3) (2011) 727-33. https://doi.org/10.1148/radiol.11100586.
5. J.H. Yoon, J.M. Lee, M. Paek, J.K. Han, B.I. Choi, Quantitative assessment of hepatic function: modified look-locker inversion recovery (MOLLI) sequence for T1 mapping on Gd-EOB-DTPA-enhanced liver MR imaging, European radiology 26(6) (2016) 1775-82. https://doi.org/10.1007/s00330-015-3994-7.
6. J.H. Yoon, J.M. Lee, E. Kim, T. Okuaki, J.K. Han, Quantitative Liver Function Analysis: Volumetric T1 Mapping with Fast Multisection B1 Inhomogeneity Correction in Hepatocyte-specific Contrast-enhanced Liver MR Imaging, Radiology 282(2) (2017) 408-417. https://doi.org/10.1148/radiol.2016152800.
7. D. Geisel, P. Raabe, L. Lüdemann, M. Malinowski, M. Stockmann, D. Seehofer, J. Pratschke, B. Hamm, T. Denecke, Measuring hepatic functional reserve using low temporal resolution Gd-EOB-DTPA dynamic contrast-enhanced MRI: a preliminary study comparing galactosyl human serum albumin scintigraphy with indocyanine green retention.
8. D. Geisel, L. Ludemann, B. Hamm, T. Denecke, Imaging-Based Liver Function Tests–Past, Present and Future, Rofo 187(10) (2015) 863-71. https://doi.org/10.1055/s-0035-1553306.
9. M. Haimerl, I. Fuhrmann, S. Poelsterl, C. Fellner, M.D. Nickel, K. Weigand, M.H. Dahlke, N. Verloh, C. Stroszczynski, P. Wiggermann, Gd-EOB-DTPA-enhanced T1 relaxometry for assessment of liver function determined by real-time (13)C-methacetin breath test, European radiology 28(9) (2018) 3591-3600. https://doi.org/10.1007/s00330-018-5337-y.
10. A. Nishie, Y. Ushijima, T. Tajima, Y. Asayama, K. Ishigami, D. Kakihara, T. Nakayama, Y. Takayama, D. Okamoto, K. Abe, M. Obara, K. Yoshimitsu, H. Honda, Quantitative analysis of liver function using superparamagnetic iron oxide- and Gd-EOB-DTPA-enhanced MRI: comparison with Technetium-99 m galactosyl serum albumin scintigraphy, Eur J Radiol 81(6) (2012) 1100-4. https://doi.org/10.1016/j.ejrad.2011.02.053.
11. D. Geisel, P. Raabe, L. Ludemann, M. Malinowski, M. Stockmann, D. Seehofer, J. Pratschke, B. Hamm, T. Denecke, Gd-EOB-DTPA-enhanced MRI for monitoring future liver remnant function after portal vein embolization and extended hemihepatectomy: A prospective trial, European radiology 27(7) (2017) 3080-3087. https://doi.org/10.1007/s00330-016-4674-y.
12. U. Motosugi, T. Ichikawa, H. Sou, K. Sano, L. Tominaga, T. Kitamura, T. Araki, Liver parenchymal enhancement of hepatocyte-phase images in Gd-EOB-DTPA-enhanced MR imaging: which biological markers of the liver function affect the enhancement?, J Magn Reson Imaging 30(5) (2009) 1042-6. https://doi.org/10.1002/jmri.21956.
13. G.M. Kukuk, S.G. Schaefer, R. Fimmers, D.R. Hadizadeh, S. Ezziddin, U. Spengler, H.H. Schild, W.A. Willinek, Hepatobiliary magnetic resonance imaging in patients with liver disease: correlation of liver enhancement with biochemical liver function tests.
14. T. Yoneyama, Y. Fukukura, K. Kamimura, K. Takumi, A. Umanodan, S. Ueno, M. Nakajo, Efficacy of liver parenchymal enhancement and liver volume to standard liver volume ratio on Gd-EOB-DTPA-enhanced MRI for estimation of liver function, European radiology 24(4) (2014) 857-65. https://doi.org/10.1007/s00330-013-3086-5.
15. K. Kamimura, Y. Fukukura, T. Yoneyama, K. Takumi, A. Tateyama, A. Umanodan, T. Shindo, Y. Kumagae, S. Ueno, C. Koriyama, M. Nakajo, Quantitative evaluation of liver function with T1 relaxation time index on Gd-EOB-DTPA-enhanced MRI:

comparison with signal intensity-based indices, J Magn Reson Imaging 40(4) (2014) 884-9. https://doi.org/10.1002/jmri.24443.
16. Y. Ding, S.X. Rao, C. Chen, R. Li, M.S. Zeng, Assessing liver function in patients with HBV-related HCC: a comparison of T(1) mapping on Gd-EOB-DTPA-enhanced MR imaging with DWI, European radiology 25(5) (2015) 1392-8. https://doi.org/10.1007/s00330-014-3542-x.
17. S. Matoori, J.M. Froehlich, S. Breitenstein, A. Doert, V. Pozdniakova, D.M. Koh, A. Gutzeit, Age dependence of spleen- and muscle-corrected hepatic signal enhancement on hepatobiliary phase gadoxetate MRI, European radiology 26(6) (2016) 1889-94. https://doi.org/10.1007/s00330-015-3965-z.
18. F. Faul, E. Erdfelder, A. Buchner, A.G. Lang, Statistical power analyses using G*Power 3.1: tests for correlation and regression analyses, Behav Res Methods 41(4) (2009) 1149-60. https://doi.org/10.3758/BRM.41.4.1149.
19. G. Nuzzo, F. Giuliante, I. Giovannini, M. Vellone, G. De Cosmo, G. Capelli, Liver resections with or without pedicle clamping, Am J Surg 181(3) (2001) 238-46.
20. G. Nuzzo, F. Giuliante, M. Vellone, G. De Cosmo, F. Ardito, M. Murazio, F. D'Acapito, I. Giovannini, Pedicle clamping with ischemic preconditioning in liver resection, Liver Transpl 10(2 Suppl 1) (2004) S53-7. https://doi.org/10.1002/lt.20045.
21. N. Verloh, M. Haimerl, F. Zeman, A. Teufel, S. Lang, C. Stroszczynski, C. Fellner, P. Wiggermann, Multivariable analysis of clinical influence factors on liver enhancement of Gd-EOB-DTPA-enhanced 3T MRI, Rofo 187(1) (2015) 29-35. https://doi.org/10.1055/s-0034-1385211.
22. D.L. Schmucker, Liver function and phase I drug metabolism in the elderly: a paradox, Drugs Aging 18(11) (2001) 837-51. https://doi.org/10.2165/00002512-200118110-00005.
23. L. Giannitrapani, M. Soresi, E. La Spada, M. Cervello, N. D'Alessandro, G. Montalto, Sex hormones and risk of liver tumor, Ann N Y Acad Sci 1089 (2006) 228-36. https://doi.org/10.1196/annals.1386.044.
24. M.W. Janssen, K.T. Druckrey-Fiskaaen, L. Omidi, G. Sliwinski, C. Thiele, B. Donaubauer, N. Polze, U.X. Kaisers, J. Thiery, C. Wittekind, J.P. Hauss, M.R. Schon, Indocyanine green R15 ratio depends directly on liver perfusion flow rate, J Hepatobiliary Pancreat Sci 17(2) (2010) 180-5. https://doi.org/10.1007/s00534-009-0160-0.
25. M.T. Inal, D. Memis, Y.A. Sezer, M. Atalay, A. Karakoc, N. Sut, Effects of intra-abdominal pressure on liver function assessed with the LiMON in critically ill patients, Can J Surg 54(3) (2011) 161-6. https://doi.org/10.1503/cjs.042709.